Hannes Prosthesis Control Based on Regression Machine Learning Algorithms

2021 IEEE/RSJ International Conference on Intelligent Robots and Systems (IROS)
September 27 - October 1, 2021. Prague, Czech Republic

Hannes Prosthesis Control Based on Regression Machine Learning Algorithms

D. Di Domenico*, A. Marinelli*, Student Member, IEEE, N. Boccardo, M. Semprini, Member, IEEE, L. Lombardi, M. Canepa, S. Stedman, A. Dellacasa Bellingegni, M. Chiappalone, Member, IEEE, E. Gruppioni, Member, IEEE, M. Laffranchi, Member, IEEE, L. De Michieli, Member, IEEE

Abstract— **The quality of life for upper limb amputees can be greatly improved by the adoption of poly-articulated myoelectric prostheses. Typically, in these applications, a pattern recognition algorithm is used to control the system by converting the recorded electromyographic activity (EMG) into complex multi-degrees of freedom (DoFs) movements. However, there is currently a trade-off between the intuitiveness of the control and the number of active DoFs. We here address this challenge by performing simultaneous multi-joint control of the Hannes system and testing several state-of-the-art classifiers to decode hand and wrist movements. The algorithms discriminated multi-DoF movements from forearm EMG signals of 10 healthy subjects reproducing hand opening-closing, wrist flexion-extension and wrist pronation-supination. We first explored the effect of the number of employed EMG electrodes on device performance through the classifiers optimization in terms of F1Score. We further improved classifiers by tuning their respective hyperparameters in terms of the Embedding Optimization Factor. Finally, three mono-lateral amputees tested the optimized algorithms to intuitively and simultaneously control the Hannes system. We found that the algorithms performances were similar to that of healthy subjects, particularly identifying the Non-Linear Regression classifier as the ideal candidate for prosthetic applications.**

I. Introduction

Myoelectric prosthetic devices represent a real opportunity for enabling upper limb amputees to perform various activities of daily living (ADLs). These prostheses typically exploit flexor and extensor muscles of the wrist through surface electromyographic (EMG) electrodes [1]. Additionally, the level of recorded muscular contraction modulates the speed of the prosthesis, implementing a proportional control [2]. Due to the high complexity of the muscular system, the relationship between EMG signals and upper limb movements is remarkably nonlinear and generally only dual-site control has been employed [3]. Moreover, the prosthesis control is narrowed to the single articulation preventing the simultaneous movement of multiple joints. Indeed, when two or more DoFs are considered, only one joint is controlled at a time, and co-contraction strategies are used to switch between DoFs [4]. Other groups have attempted the direct control of multi-DoF prostheses by implementing a multi amplitude strategy using dual-site electrodes, by thresholding the muscle contraction intensity [5]. However, this strategy is not intuitive, with movements appearing to be clumsy and unnatural, therefore preventing users from feeling the prosthesis as part of their body [6]. In order to overcome these limits, pattern recognition algorithms were adopted by many groups to decode the intended movement, with the final goal of increasing the controllability of multi-DoF prosthetic devices [7-9]. However, current pattern recognition approaches demonstrated poor performance with DoFs higher than 2 [10]. Another limitation of these studies is that the outcomes achieved during laboratory experiments are poorly assessed in real ADL applications [2]. Therefore, there is an urgent need of a reliable and stable classifier able to deal with unknown situations typical of ADLs [11-14]. We addressed this challenge by implementing a pattern recognition control specifically optimized for the Hannes system, a novel poly-articulated hand prosthesis [15], to generate a robust, intuitive and human-like simultaneous DoFs control. Concerning the previous work where only hand opening and closing were actively controlled [15], we here include the classification of other two DoFs of the wrist. We optimized and tested several pattern recognition algorithms that process information coming solely from the EMG electrodes embedded in the prosthetic device. We then implemented the resulting best performing algorithm for simultaneous online control of the Hannes system joints. Our group already tested pattern recognition algorithms for translating muscular activity into virtual hand movements in 2 DoFs only (rest, hand opening-closing (HOC), wrist pronation-supination (WPS)) [16]. We here extend this work by including the detection of wrist flexion-extension (WFE) for the real-time control of the Hannes prosthesis [16]. We assessed the performance of the detection algorithms for the control of the Hannes prosthetic hand both with 10 healthy subjects and with 3 trans-radial

Research supported by INAIL, grant PPR-AS 2017-2020.

* These authors equally contributed to this work.

D. Di Domenico, A. Marinelli, N. Boccardo, M. Semprini, L. Lombardi, M. Canepa, S. Stedman, M. Chiappalone, E. Gruppioni, M. Laffranchi, L. De Michieli are with the Rehab Technologies Lab, Istituto Italiano di Tecnologia, Genova 16163 Italy (Tel.: 0039-010-28961; e-mails: dario.didomenico@iit.it, andrea.marinelli@iit.it, nicolo.boccardo@iit.it, marianna.semprini@iit.it, lorenzo.lombardi@iit.it, michele.canepa@iit.it, samuel.stedman@iit.it, michela.chiappalone@iit.it, matteo.laffranchi@iit.it, lorenzo.demichieli@iit.it).

A. Marinelli is also with the Department of Informatics, Bioengineering, Robotics and systems Engineering, University of Genova, 16145 Italy.

A. Dellacasa Bellingegni and E. Gruppioni are with the Prosthetic Centre INAIL, Vigorso di Budrio, Bologna 40054 Italy (e-mails: a.dellacasabellingegni@inail.it, e.gruppioni@inail.it).

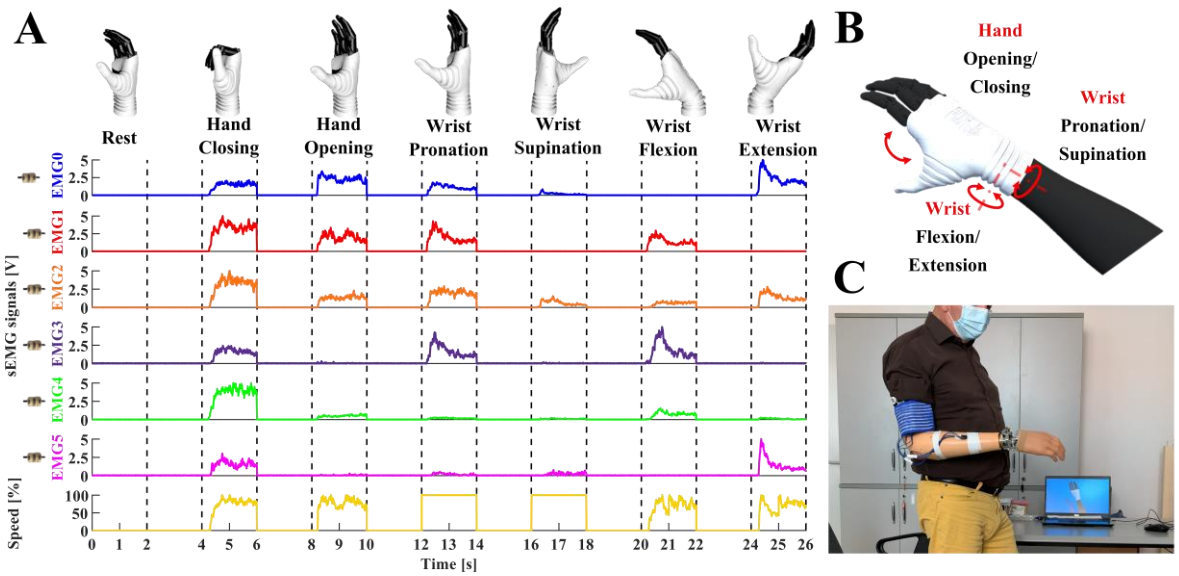

Figure 1. sEMG activities related to each gesture. **A**: EMG signals and Hannes system speed during different gestures. **B**: available degrees of freedom of the Hannes system. **C**: Amputee performing Real-Time control of Hannes and VR.

amputees. The examined classifiers were: Non-Linear Logistic Regression (NLR) [17], Regularized Least-Square (RLS) [18], Artificial Neural Network (ANN) [19], Support Vector Machine (SVM) [20], and Linear Discriminant Analysis (LDA) [17]. For NLR, RLS and LDA methods, we combined pattern recognition with an "abstention" criterion. This consists in evaluating the likelihood of the decoded joint movement and enabling an "abstention" criterion (i.e. confidence-based rejection) [21]. The hyperparameters calibration and the integration of abstention inside each algorithm greatly improved the classifier accuracy. The increased number of DoFs to be simultaneously classified could lead to lower algorithms accuracy with respect to simpler settings [15, 16], nevertheless we here show that performances were still suitable for prosthetic control. We also found that both for amputees and able-bodied subjects, the NLR outperformed the other classifiers.

II. Materials and Methods

A. Subjects

We involved ten healthy subjects aged between 22 and 33 years (27.1 ± 3.2) and three mono-lateral amputees (trans-radial amputation of the dominant limb, already users of active prostheses). Written informed consent was obtained from all subjects. The study adhered to the standard of the Declaration of Helsinki and was approved by the Bologna-Imola ethical committees (CP-PPRAS1/1-01).

B. Experimental Protocol

Six Ottobock EMG electrodes (13E200=50 AC) were attached to an elastic band (Fig. 2 A) wrapped around the forearm or stump approximately 5cm distal to the olecranon. These electrodes measured muscular electrical activities during grasping, WPS and WFE movements (Fig. 1 A). Muscles involved were identified by manual inspection and they were: Extensor Carpi Radialis Longus (EMG_0), Extensor Digitorum (EMG_2), Extensor Carpi Ulnaris (EMG_4), Palmaris Longus and Flexor Carpi Ulnaris (EMG_1), Flexor Carpi Radialis (EMG_3) and the Brachioradialis Muscle (EMG_5).

After electrodes positioning, users were placed in front of a display showing the virtual Hannes system (Fig. 2 E). We required subjects to sequentially execute HOC, WPS and WFE 10 times. Then, we also recorded 16 repetitions of resting position (2s time-window and 1kHz sampling frequency) and combined their samples into a random distribution, obtaining a total of 24 repetitions (4 repetitions x 6 gestures). This resting data was then randomly arranged for each gesture to create an indecision region.

C. Processing of EMG signals

EMG signals followed the same processing already described in [16]. Briefly, a custom EMG-master board implements the A/D conversion of the input data, which are subsequently sent to the PC via Bluetooth. We then used a customized version of the EMG - Data Acquisition & Training Software (E-DATS [16, 17], Fig. 2 E) to both collect data and offline train the algorithms. The model generation was realized through a MATLAB script (MathWorks).

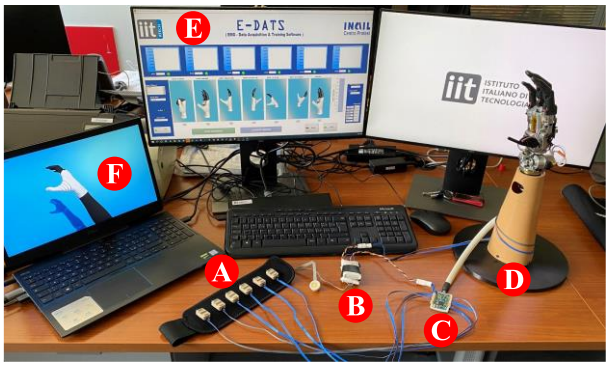

Figure 2. Experimental Setup. **A**: EMG electrodes, **B**: power supply, **C**: EMG processing board, **D**: Hannes system, **E**: E-DATS software, **F**: Hannes system in a non-immersive virtual-reality on Unity.

Following classifier training, real-time recognition of the available gestures was performed. Afterward, the Hannes system, equipped with the resulting best classifier, was controlled in real-time by each subject.

D. Train and test the algorithms

Algorithms (see paragraph II.F) were first calibrated, in order to obtain internal parameters able to satisfy high performances with the lowest computational effort during the online control, as detailed in [16]. For the LDA algorithm, we split the dataset into a training set (70% of the data) and a test set (30% of the data). The other algorithms were used after down-sampling the data from 1kHz to 40Hz, obtaining a training group (4% of the data) and a test set (96% of the data). The training group was in turn divided into a training set (2.4% of the data for offline tuning of the internal parameters), validation set (0.8% of the data for tuning the hyperparameters to prevent overfitting), and threshold optimization set (0.8% of the data for tuning the likelihood threshold for the abstention criterion). Afterward, we used the resulting best algorithm, already calibrated, for online decoding of hand motion using a real-time PC simulation based on pattern recognition (Model evaluation in Fig. 3). The optimized model was then uploaded (Model upload in Fig. 3) to the EMG processing board (TiVa Cortex-M4) for final online classification (Hannes in Fig. 3), used to freely control the Hannes with sampling frequency set to 300Hz.

E. Hannes hand

The Hannes prosthetic system consists of: (i) a set of six EMG electrodes, (ii) a custom EMG processing unit, (iii) a myoelectric poly-articulated prosthetic hand (Fig. 2 D), (iv) an active WFE, (v) an active WPS, and (vi) a battery pack (Fig. 2 B). The EMG processing unit ("EMG-Master" Fig. 2 C) acquires the analog sensor output and synthesizes the control signals for each active joint. The extent of the activation is proportional to the RMS of the six EMG signals, normalized in the range 0 to 100%. An exception is the WPS, which is always controlled at the maximum velocity. The references are then sent to the respective motor control boards within the prosthetic system. Each motor driver has an on-board control loop to ensure the correct joint movement: closed-loop speed control for the hand and WFE, and open-loop for the WPS. A detailed description of the mechanical design of the prosthetic hand is provided in [15]. To the architecture described in [15], the current system adds the two active DoFs for the wrist. The WFE consists of a custom drivetrain based on a worm gear, ideal to withstand the high external loads. The overall range of motion achieved is ±65°. Similarly, the WPS consists of a standard motor-gearbox actuation and it can provide 360° rotation. The "de-facto" standard quick disconnect system by Ottobock was replicated, as described in [15].

F. Algorithms and hyperparameters optimization

Following previous work on prosthetic control [13], we compared supervised machine learning algorithms: NLR [17], RLS [18], ANN [19], SVM [20], and LDA [17]. We first estimated the minimum number of EMG electrodes for each classifier by computing, for each configuration of EMG

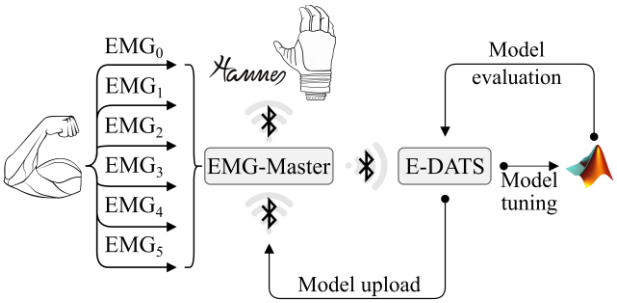

Figure 3. Diagram of the model generation and Hannes control.

sensors, the F1Score performance. For the NLR classifier, we optimized the polynomial degree (D), which plays an important role since it represents the complexity of the algorithm, as described in [16]. The higher the complexity, the greater the computational burden required to the processing board. Regarding the ANN, we investigated the importance of the number of hidden layers by fixing the number of neurons to the highest value (30) and then we optimized the number of neurons, considering the previously obtained optimal number of hidden layers. Furthermore, in RLS, LDA and NLR, the maximization of the voluntary gestures recognition was implemented through the addition of a Likelihood threshold [13]. The threshold, ranging between 0.7 and 1, was optimized for each subject and each algorithm in terms of F1Score [22]. During offline optimization, in the cases of movements under threshold or simultaneous supra-threshold movements, the classifier abstained without classifying. During online classification, supra-threshold movements belonging to the same DoF were considered as "abstentions", while supra-threshold movements belonging to different DoFs produced simultaneous movements. We used the test set (paragraph II.D) to assess the performance of each algorithm in terms of F1Score and Embedding Optimization Factor (EOF), considering different configurations of hyperparameters. The EOF explains the trade-off between performance accuracy and complexity of the algorithm, which is strongly related to the computational burden on the EMG processing board [17]. This index is associated to the available memory on the EMG-Master. Therefore, it may happen that in some cases (e.g. full configuration of EMG sensors), the model has too many parameters for the available flash memory, resulting in EOF obtaining negative scores (see [17] for EOF calculation). We compared the performance of each algorithm in terms of F1Score, EOF, classification (percentage of correctly decoded movements, i.e. accuracy), and abstention (percentage of not assigned movements). Afterward, the optimized hyperparameters were exploited to build optimal classifiers on the amputees dataset. We used Wilcoxon-Signed-Rank test and Bonferroni correction [23] for statistical analysis.

III. Results

A. Variation of EMG electrodes number

The minimum number of EMG electrodes was first determined to optimize the performance of each algorithm, highlighted by the absence of statistical difference in the

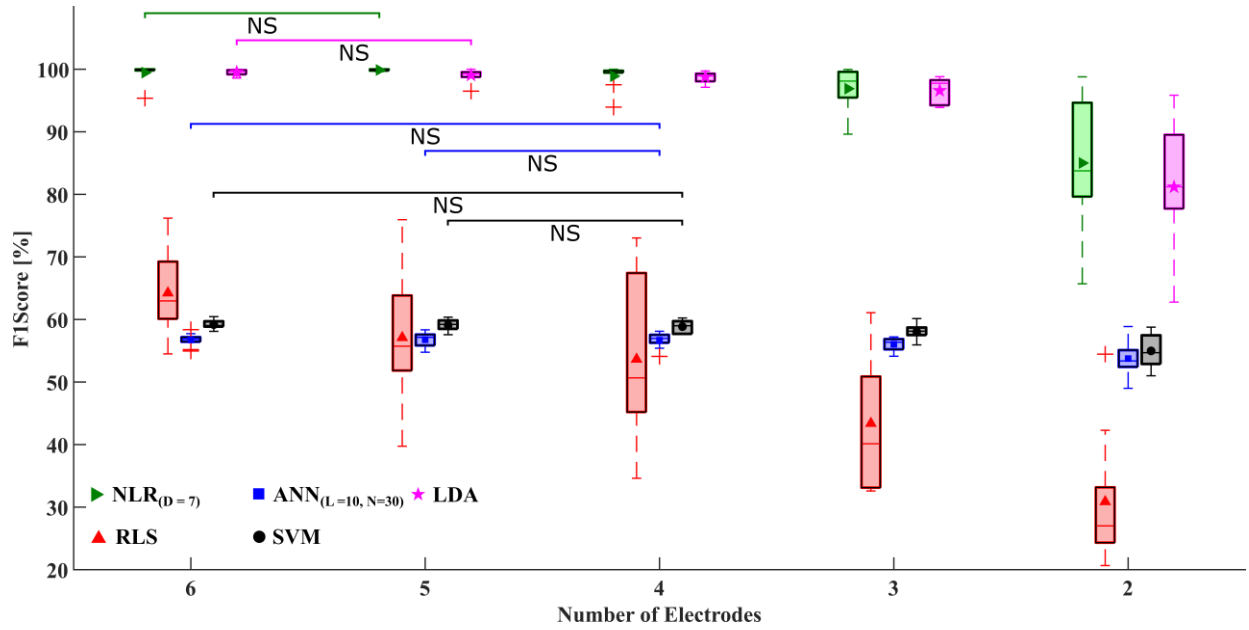

Figure 4. Performance of F1Score when varying the number of electrodes for each classifier. In the NLR the D-value is fixed to 7, while for ANN the number of hidden layers is 10 and the number of neurons is 30. NS: not significant.

F1Score (NS in Fig. 4). Then, starting from the setup with 6 EMG electrodes, we successively decreased the number of sensors by ignoring EMG signals coming from muscles with lower activity, according to the following order: EMG_5, EMG_2, EMG_3, EMG_4. Regarding the LDA and the NLR classifier, the best configuration was obtained either with five or six electrodes. For SVM and ANN, only four electrodes were required to maximize the performance, while for RLS the full configuration with 6 EMG sensors saturated the performance. However, F1score was highest for NRL and LDA with any configuration of electrodes, while in other cases, it was always lower than 65%.

B. NLR: variation of polynomial degree D

Regarding the NLR classifier, we swept the polynomial degree (D-value) in the range 1-7 to assess the performance in terms of EOF. As represented in Fig. 5, we obtained the optimal behavior for D = 2.

C. ANN: variation of network architecture

Concerning the ANN classifier, we evaluated how the number of hidden layers affects performance using a configuration of 4 EMG electrodes. We tested the EOF performance when varying the number of hidden layers (L) from 1 to 10 (according to [17]) and keeping fixed to 30 the number of neurons. We found optimal EOF values with L=5 or greater (Fig. 6 A). Subsequently, we considered as the optimal choice L = 5 and we varied the maximum number of neurons (N) between: [1, 5, 10, 15, 20, 23, 24, 25, 26, 27, 28, 29, 30]. We compared the performance of the different configurations to establish the best hyperparameters setup. We set N=1 since we found that performances do not degrade when considering more neurons (Fig. 6 B).

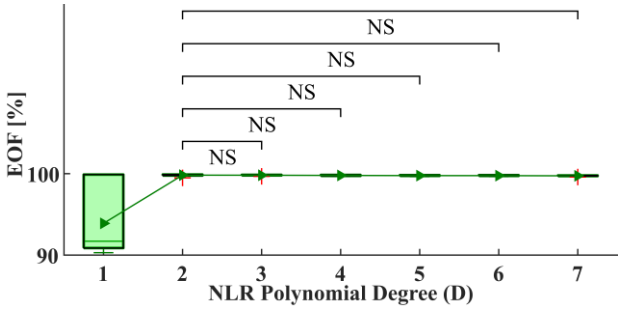

Figure 5. NLR optimization with 5 electrodes: EOF performance when varying the maximum D-value. NS: not significant.

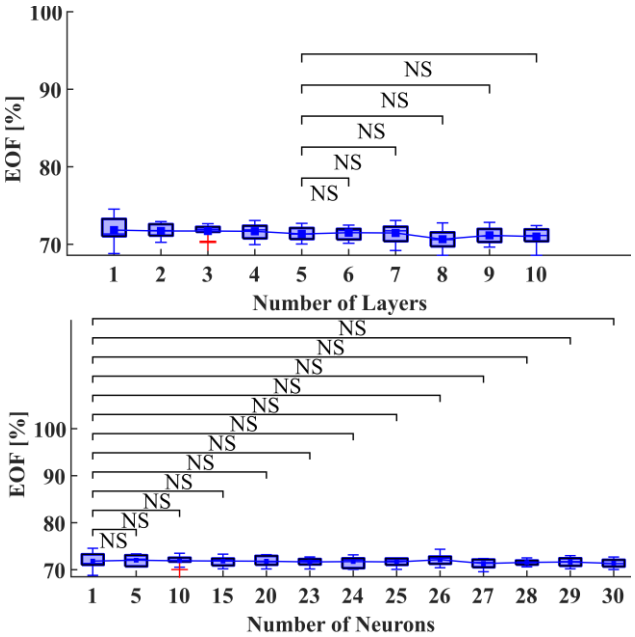

Figure 6. ANN optimization with 4 EMG sensors. **A**: EOF performance when the maximum number of hidden layers varies and the maximum number of neurons is fixed to 30. **B**: EOF performance when the maximum number of neurons varies and the maximum number of hidden layers is fixed to 5. NS: not significant.

D. *Analysis of algorithms performance*

Fig. 7 highlights the behavior of the classifiers in terms of F1Score, EOF, classification, and abstention obtained by the various algorithms in their optimized configurations (i.e. optimal values of hyperparameters). With respect to F1Score, EOF and classification (Fig. 7 A, B and C), NLR always reached the highest value. Although the F1Score has no statistical difference between NLR and LDA (gold standard), the former obtained less dispersed results, as indicated by small standard deviation. However, the highest abstention was reached by NLR (Fig. 7 D).

E. *Tests on amputees*

With trans-radial amputees, we used the optimal configurations of the classifiers obtained from the analysis on able-bodied subjects. Moreover, we compared the performance obtained by amputees with those of the healthy subjects to assess whether the algorithms perform differently in the two cases. TABLE I highlights the values of F1Score, EOF, classification, and abstention achieved by amputees. Scores of the patients matched those obtained by able-bodied subjects: NLR had the highest classification score, followed by LDA. F1Scores and EOF were highest for NLR, followed by LDA for patients #1 and #3, vice versa for the other subject. NLR obtained greater abstentions. During the experiments, the amputees verbally expressed their satisfaction towards the improved controllability of the tested system with respect to their usual prosthesis.

IV. Discussion

We tested multiple supervised machine learning algorithms to decode prosthesis movements. We found NLR and LDA algorithms as top performers, with respect to EOF, with a configuration of 5 EMG electrodes. In a previous study including only 1 DoF for the wrist [16], our group found that 3 EMG electrodes were enough for NLR to reach top performance. We here show that the successful decoding of 3 DoFs movements came at the cost of increasing the number of EMG electrodes needed (from 3 to 5). NLR maintained the same performance when the degree of polynomial complexity is higher or equal than 2. This guarantees that the computational burden is still kept at a minimum, even with a greater number of decoded classes, with respect to [16]. Regarding the ANN algorithm, we optimized the architecture of the network with respect to our previous study [16]. Indeed, the optimal maximum number of hidden layers decreased to 5 (6 in [16]) and that of neurons decreased to 1 (24 in [16]). However, the performances dramatically dropped as both classification and F1scores decreased to 51.3% and 56.1%, respectively (80.3% and 80.2%, respectively, in [16]), presumably as an effect due to the increased number of decoded classes that causes less separation of gestures into the parameter hyperspace. Differently from [10], where they achieved degraded performance for the 3-DoFs control, we here discovered that, with the same number of DoFs, the NLR algorithm is the most suitable for a prosthesis control based on pattern recognition. Although no statistical difference was found between NRL and LDA algorithms, NRL showed smaller standard deviations (see Fig. 7 A). NLR and LDA

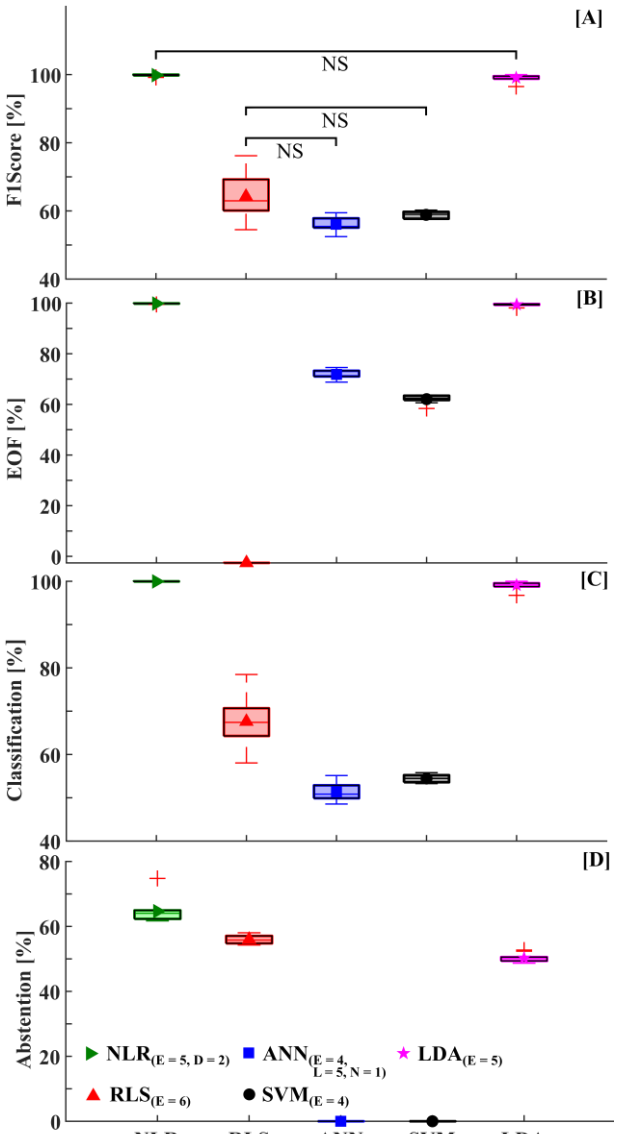

Figure 7. Algorithms comparison. **A**: Performance of F1Score. **B**: EOF index. **C**: Percentage of correctly classified outputs. **D**: Percentage of abstention. NS: not significant.

were also the best performing algorithms for amputees, who succeeded in the control of the Hannes system through the residual muscular activity of the stump. With respect to other classifiers, NLR also reached a higher percentage of abstentions. Nonetheless, due to the high classification frequency, set to 300Hz, 300 movements per second were decoded. Consequently, latency between movement intentions and resulting action was not perceived by users even in case of high abstention rate. The abstention criterion reduced the number of classification artifacts, leading to more robust and consistent classification with respect to the state of the art systems in a similar context [24, 25]. The NLR algorithm was therefore implemented on the microcontroller board for online control of Hannes. Subjects could then freely explore the human-like behavior of the system, which was able to achieve simultaneous and intuitive control of multi-DoFs, a fundamental feature for bioinspired prosthetic use, not yet achieved by current state-of-the-art systems [2, 25]. Indeed, as reported by amputees, the NLR classifier allows

TABLE I: AMPUTEES RESULTS. In bold are highlighted the best performances of each index (F1Score, EOF, classification, and abstention) for each amputee. The number of electrodes is fixed from the results on the able-bodied subjects.

S.	*Alg.*	*EMG sensors*	*F1Score [%]*	*EOF [%]*	*Classification [%]*	*Abstention [%]*
1	*NLR*	5	**99.73**	**99.77**	**99.96**	**82.21**
	RLS	6	38.22	-2.62	42.27	52.99
	ANN	4	54.63	70.64	49.21	-
	SVM	4	59.37	61.86	55.06	-
	LDA	5	97.86	98.80	98.51	57.88
2	*NLR*	5	93.81	96.71	**98.91**	**77.95**
	RLS	6	35.09	-2.63	37.47	56.04
	ANN	4	44.45	61.54	41.70	-
	SVM	4	50.88	54.23	47.54	-
	LDA	5	**94.73**	**97.18**	94.59	54.88
3	*NLR*	5	**99.91**	**99.86**	**99.99**	**77.08**
	RLS	6	44.75	-2.61	48.12	56.82
	ANN	4	49.29	66.02	44.61	-
	SVM	4	55.31	59.28	51.64	-
	LDA	5	96.46	98.08	96.69	53.63

the reliable translation of the gesture intentions into actual movements (Fig. 1 C). However, online control was not systematically tested as for the offline phase, leaving online control to be further assessed in future experiments. Moreover, we need to increase the number of amputated subjects in order to properly perform statistical analysis. Finally, to truly assess the validity of NLR for simultaneous multi-joint prosthetic control, it will be fundamental to perform tests outside the lab and in the context of ADLs.

V. CONCLUSION

We here assessed the ability of multiple supervised machine learning algorithms to simultaneously control upper limb prosthesis through EMG signals detected at the forearm level of healthy subjects. NLR turns out to be the best operating algorithm and we further supported this result by tests on trans-radial amputees controlling the Hannes system (see the attached VIDEO). We will now extend this study to a wider amputees population in the context of ADLs, in order to truly test NLR control of prosthetic devices in real life context.

REFERENCES

[1] C. J. De Luca, "The use of surface electromyography in biomechanics," *Journal of applied biomechanics,* vol. 13, no. 2, pp. 135-163, 1997.

[2] A. D. Roche, B. Lakey, I. Mendez, I. Vujaklija, D. Farina, and O. C. Aszmann, "Clinical perspectives in upper limb prostheses: An update," *Current Surgery Reports,* vol. 7, no. 3, p. 5, 2019.

[3] P. K. Artemiadis and K. J. Kyriakopoulos, "An EMG-based robot control scheme robust to time-varying EMG signal features," *IEEE Transactions on Information Technology in Biomedicine,* vol. 14, no. 3, pp. 582-588, 2010.

[4] I. Vujaklija, D. Farina, and O. C. Aszmann, "New developments in prosthetic arm systems," *Orthopedic research and reviews,* vol. 8, p. 31, 2016.

[5] M. Markovic, M. Varel, M. A. Schweisfurth, A. F. Schilling, and S. Dosen, "Closed-loop multi-amplitude control for robust and dexterous performance of myoelectric prosthesis," *IEEE Transactions on Neural Systems and Rehabilitation Engineering,* vol. 28, no. 2, pp. 498-507, 2019.

[6] A. Chadwell, L. Kenney, S. Thies, A. Galpin, and J. Head, "The reality of myoelectric prostheses: understanding what makes these devices difficult for some users to control," *Frontiers in neurorobotics,* vol. 10, p. 7, 2016.

[7] M. Sartori, G. Durandau, S. Došen, and D. Farina, "Robust simultaneous myoelectric control of multiple degrees of freedom in wrist-hand prostheses by real-time neuromusculoskeletal modeling," *Journal of neural engineering,* vol. 15, no. 6, p. 066026, 2018.

[8] J. M. Hahne, M. A. Schweisfurth, M. Koppe, and D. Farina, "Simultaneous control of multiple functions of bionic hand prostheses: Performance and robustness in end users," *Science Robotics,* vol. 3, no. 19, p. eaat3630, 2018.

[9] T. Kapelner, F. Negro, O. C. Aszmann, and D. Farina, "Decoding motor unit activity from forearm muscles: perspectives for myoelectric control," *IEEE Transactions on Neural Systems and Rehabilitation Engineering,* vol. 26, no. 1, pp. 244-251, 2017.

[10] C. Piazza, M. Rossi, M. G. Catalano, A. Bicchi, and L. J. Hargrove, "Evaluation of a Simultaneous Myoelectric Control Strategy for a Multi-DoF Transradial Prosthesis," *IEEE Transactions on Neural Systems and Rehabilitation Engineering,* 2020.

[11] A. J. Young, L. J. Hargrove, and T. A. Kuiken, "The effects of electrode size and orientation on the sensitivity of myoelectric pattern recognition systems to electrode shift," (in eng), *IEEE Trans Biomed Eng,* vol. 58, no. 9, pp. 2537-44, Sep 2011, doi: 10.1109/TBME.2011.2159216.

[12] B. Wan *et al.*, "Study on fatigue feature from forearm SEMG signal based on wavelet analysis," in *2010 IEEE International Conference on Robotics and Biomimetics*, 2010: IEEE, pp. 1229-1232.

[13] S. Amsüss, P. M. Goebel, N. Jiang, B. Graimann, L. Paredes, and D. Farina, "Self-correcting pattern recognition system of surface EMG signals for upper limb prosthesis control," *IEEE Transactions on Biomedical Engineering,* vol. 61, no. 4, pp. 1167-1176, 2013.

[14] C. Castellini, A. E. Fiorilla, and G. Sandini, "Multi-subject/daily-life activity EMG-based control of mechanical hands," *Journal of neuroengineering and rehabilitation,* vol. 6, no. 1, pp. 1-11, 2009.

[15] M. Laffranchi *et al.*, "The Hannes hand prosthesis replicates the key biological properties of the human hand," *Science Robotics,* vol. 5, no. 46, p. eabb0467, 2020, doi: 10.1126/scirobotics.abb0467.

[16] A. Marinelli *et al.*, "Performance Evaluation of Pattern Recognition Algorithms for Upper Limb Prosthetic Applications," in *8th IEEE RAS/EMBS International Conference for Biomedical Robotics and Biomechatronics (BioRob)*, 2020: IEEE, pp. 471-476.

[17] A. Dellacasa Bellingegni *et al.*, "NLR, MLP, SVM, and LDA: a comparative analysis on EMG data from people with trans-radial amputation," *J Neuroeng Rehabil,* vol. 14, no. 1, p. 82, Aug 14 2017, doi: 10.1186/s12984-017-0290-6.

[18] H. Sun and Q. Wu, "Regularized least square regression with dependent samples," *Advances in Computational Mathematics,* vol. 32, no. 2, pp. 175-189, 2010.

[19] S. Dreiseitl and L. Ohno-Machado, "Logistic regression and artificial neural network classification models: a methodology review," *Journal of biomedical informatics,* vol. 35, no. 5-6, pp. 352-359, 2002.

[20] C.-C. Chang and C.-J. Lin, "LIBSVM: A library for support vector machines," *ACM transactions on intelligent systems and technology (TIST),* vol. 2, no. 3, pp. 1-27, 2011.

[21] J. W. Robertson, K. B. Englehart, and E. J. Scheme, "Effects of confidence-based rejection on usability and error in pattern recognition-based myoelectric control," *IEEE journal of biomedical and health informatics,* vol. 23, no. 5, pp. 2002-2008, 2018.

[22] D. M. Powers, "Evaluation: from precision, recall and F-measure to ROC, informedness, markedness and correlation," 2011.

[23] J. Demšar, "Statistical comparisons of classifiers over multiple data sets," *Journal of Machine learning research,* vol. 7, no. Jan, pp. 1-30, 2006.

[24] S. Amsuess *et al.*, "Context-dependent upper limb prosthesis control for natural and robust use," *IEEE Transactions on Neural Systems and Rehabilitation Engineering,* vol. 24, no. 7, pp. 744-753, 2015.

[25] I. Kyranou, S. Vijayakumar, and M. S. Erden, "Causes of performance degradation in non-invasive electromyographic pattern recognition in upper limb prostheses," *Frontiers in neurorobotics,* vol. 12, p. 58, 2018.